

Photon and dilepton production in high energy heavy ion collisions

TAKAO SAKAGUCHI^{a,*}^aPhysics Department, Brookhaven National Laboratory, Upton, NY 11973-5000, USA

Abstract. The recent results on direct photons and dileptons in high energy heavy ion collisions, obtained particularly at RHIC and LHC are reviewed. The results are new not only in terms of the probes, but also in terms of the precision. We will discuss the physics learned from the results.

Keywords. Photons, Dileptons, RHIC, LHC, QGP

PACS Nos. 25.75.-q, 25.75.Bh, 25.75.Cj, 25.75.Nq

1. Introduction

Electromagnetic radiations are an excellent probe for extracting thermodynamical information of a matter produced in nucleus-nucleus collisions, as they are emitted from all the stages of collisions with wide Q^2 , and don't interact strongly with medium once produced [1]. They appear in two figures, namely, photons (γ) that have zero-mass and virtual photons (γ^*) that have finite mass. Experimentalists often refer virtual photons as dileptons since they have been measuring virtual photons through lepton-pair channels ($\gamma^* \rightarrow ee, \mu\mu$), by which a wide kinematic range in invariant mass and transverse momentum (p_T) can be explored. Photons are produced through a Compton scattering of quarks and gluons ($qg \rightarrow q\gamma$) or an annihilation of quarks and anti-quarks ($q\bar{q} \rightarrow g\gamma$) as leading-order (LO) processes, and the next-to-leading order (NLO) process is dominated by Bremsstrahlung and fragmentation ($qg \rightarrow qq\gamma$), as depicted in Figure 1. Their

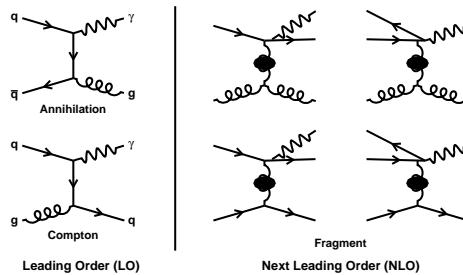


Figure 1. Production processes of direct photons.

*takao@bnl.gov

yields are proportional to $\alpha\alpha_s$, which are ~ 40 times lower than those of hadrons that are produced in strong interactions. Virtual photons are produced by annihilation of quarks and anti-quarks. The initial hard scattering process that takes place in the beginning of the collisions produces relatively high p_T photons, often referred as hard photons. They have same LO and NLO processes, and are called prompt photons and fragment photons, respectively. The production rate of these photons are well described by a NLO pQCD calculation [2]. Photons will be emitted from the hot and dense medium (quark-gluon plasma: QGP) in high energy nucleus collisions and manifest at moderate p_T ($1 < p_T < 3 \text{ GeV}/c$) if the QGP is formed [3]. We often call these photons as thermal photons. The thermal photons are of interest in exploring thermodynamical nature of the QGP, such as temperature. One can also obtain the degree of freedom of the system by combining the temperature with measurement of the energy density of the system as $g \propto \epsilon/T^4$. For $p_T < 1 \text{ GeV}$, the photons are predominantly contributed from hadron gas state via the processes of $\pi\pi(\rho) \rightarrow \gamma\rho(\pi)$, $\pi K^* \rightarrow K\gamma$ and etc., which are no longer the quark-gluon level interaction. We often refer these photons as hadron-gas photons. Photons from Compton scattering of hard-scattered partons and partons in the medium (jet-photon conversion), or Bremsstrahlung of the hard scattered partons in the medium have been predicted to contribute in the p_T range of $p_T > 2.5 \text{ GeV}/c$ if QGP is created [4]. Figure 2 shows a landscape of photon sources as a function of formation time and p_T . As described above, photons have rich information on the state they are emitted. How-

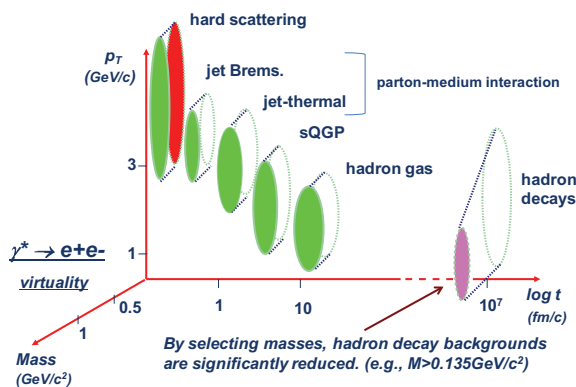


Figure 2. Manifestation of photons from various sources as a function of formation time and p_T .

ever these photons are overwhelmed by the large background coming from the decay of hadrons. $\pi^0 \rightarrow \gamma\gamma$ and $\eta \rightarrow \gamma\gamma$ are the major contributors to the background ($\sim 95\%$). The signal to background ratio at 1-3 GeV/c is of the order $\sim 10\%$. One can understand the difficulty of the measurement by comparing the uncertainty of the best π^0 measurement at RHIC [5] which directly relates to the precision of background determination. There is a certain probability that photons produced by the same process acquire virtual mass and decay into lepton-pairs (shown as one another degree of freedom in Figure 1(b)). This process is called internal conversion process and is different from the virtual photon production described above. We will explain these photons in detail in a later section. There have been several attempts on measuring thermal photons in high energy nuclear collisions as an evidence of QGP formation. The first sizable signal was reported by the WA98 experiments at SPS in $1 < p_T < 3 \text{ GeV}/c$ where a calculation predicts that QGP photons manifest [6]. At that time, the hard photons were not measured

because the statistics ran out at the p_T where the hard photons start arising. Estimating the hard photon contribution had to rely on a theoretical guidance that had large ambiguity, therefore the measurement was not able to exhibit the thermal photon contribution [3].

The source of dileptons depend on their mass and p_T of the measurement. The low mass region ($m_{ee} < 1 \text{ GeV}/c^2$) at low p_T is predominantly from the in-medium decay of ρ mesons and/or thermal radiation as shown in Figure 3(a) [7]. The same mass region at

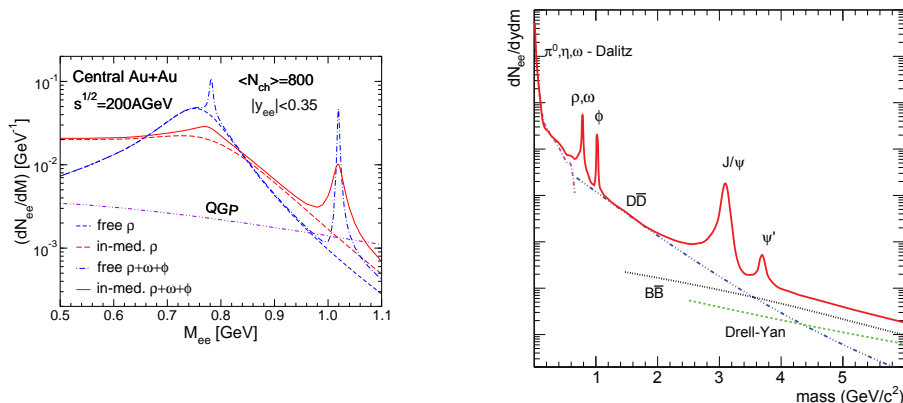


Figure 3. (a, left) A calculation of dilepton source in low mass region. (b, right) Outline of background components and resonances in dilepton invariant mass spectra.

higher p_T or higher mass region at lower p_T are from mainly from the thermal radiation. The dileptons of interest are obtained after subtracting large combinatoric background arising from Dalitz decays of π^0 or η (e.g., $\pi^0, \eta \rightarrow e^+e^-\gamma$). The outline of the background components and resonances in dilepton mass spectra is shown in Figure 3(b) [8].

In this paper, we review the recent measurements of photons and dileptons from RHIC and LHC experiments and discuss what we have learned from the data.

2. Hard production of photons and dileptons

One of the big success in electromagnetic radiation measurements in relativistic heavy ion collisions is the observation of high p_T direct photons that are produced in initial hard scattering [9]. Figure 4(a) and (b) show the latest direct photon p_T spectra in Au+Au collisions at $\sqrt{s_{NN}}=200 \text{ GeV}$ for various centralities, and the nuclear modification factor (R_{AA}) for the 0-10% centrality, respectively [10]. The R_{AA} is consistent with unity within quoted uncertainty, implying that the photons from Au+Au collisions are consistent with ones expected from $p + p$ collisions. This result is not very trivial since photons from hard scattering include both prompt and fragment components. The fragment photons may be reduced in central Au+Au collisions due to the parton energy loss. The data is compared with several model predictions. It is interesting to note that a model that includes reduction of fragment photon due to energy loss of hard scattered partons and increase of jet-photon conversion photons (coherent + conversion + ΔE) is not consistent with the data. The small suppression in R_{AA} seen in the highest p_T is likely due to the fact that the ratio of the yields in Au+Au to $p + p$ was computed without taking the isospin dependence of direct photon production into account [11]. The LHC heavy ion runs have the cms energy of 2.76 TeV where the hard photon production is copious. One

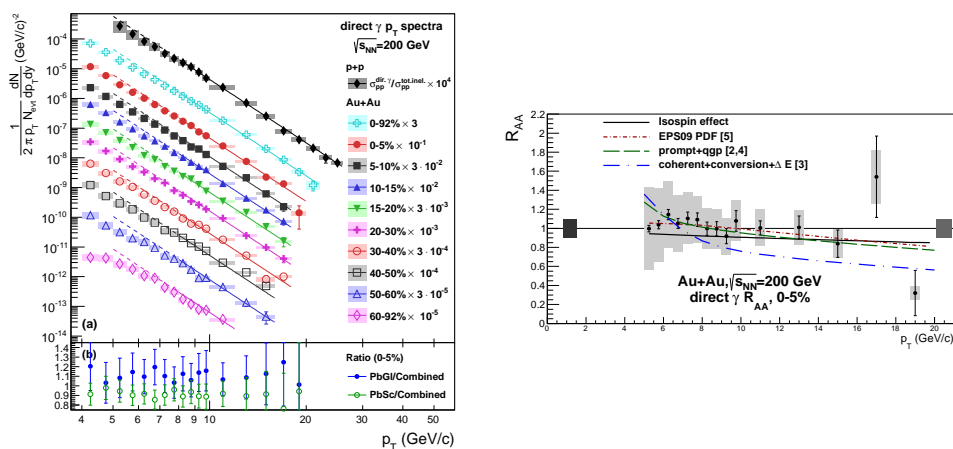


Figure 4. (a, left) Direct photon p_T spectra in Au+Au collisions at $\sqrt{s_{NN}}=200$ GeV measured by the PHENIX experiment. (b, right) Nuclear modification factor (R_{AA}) for direct photons in 10 % central Au+Au collisions [10].

can make a photon isolation cut to enrich the prompt photon component even in heavy ion collisions. Figure 5(a) shows the isolated photon p_T distributions in Pb+Pb collisions at $\sqrt{s_{NN}}=2.76$ TeV measured by the ATLAS experiment at LHC, together with ones by the CMS experiments [12, 13]. The lines show the expected values from Jet-Phox and PYTHIA event generators. The prompt photon component should be unaffected by the medium created in heavy ion collisions, and was experimentally confirmed by these measurements. Considering the fact that neither prompt photons from LHC nor prompt+fragment photons from RHIC are suppressed, the contribution of photons from fragmentation and jet-photon conversion could be smaller than predicted. Several measurements benefited from the fact that these hard electromagnetic radiations are well under control. For instance, direct photons are utilized to quantify jet energy loss as they carry the initial momenta of jets [12, 14]. A new hard probe that became available at the LHC energy is Z -bosons. The Z -bosons have a peak mass of ~ 80 GeV/ c^2 , and are produced in the medium with a lifetime of 0.1 fm/ c . Therefore, they carry information on the initial states of the collisions, and decay before they are affected by the medium. The Z -boson yields scaled by nuclear thickness function (T_{AB}) as a function of N_{part} (centrality) published by the CMS experiments are shown in Figure 5(b) [15]. The similar results are recently published by the ATLAS experiments [16]. The Z -boson yields are found to follow the scaling of the initial hard scattering process. Z -boson is also ideal for serving as a reference in many similar measurements, such as Z -jet correlations [17]. We point out that Z -bosons can serve as one of the most reliable tools to normalize the dilepton spectra between $p + p$ and A+A collisions.

3. Thermal photon production

3.1 Spectra

In the conventional real photon measurement, single photons can be observed after a huge amount of background photons coming from hadron decays (π^0 , η , η' and ω , etc.) are subtracted off from the inclusive photon distributions. This fact makes it very difficult to look at the signal at low p_T , where thermal photons from QGP manifest. A breakthrough was

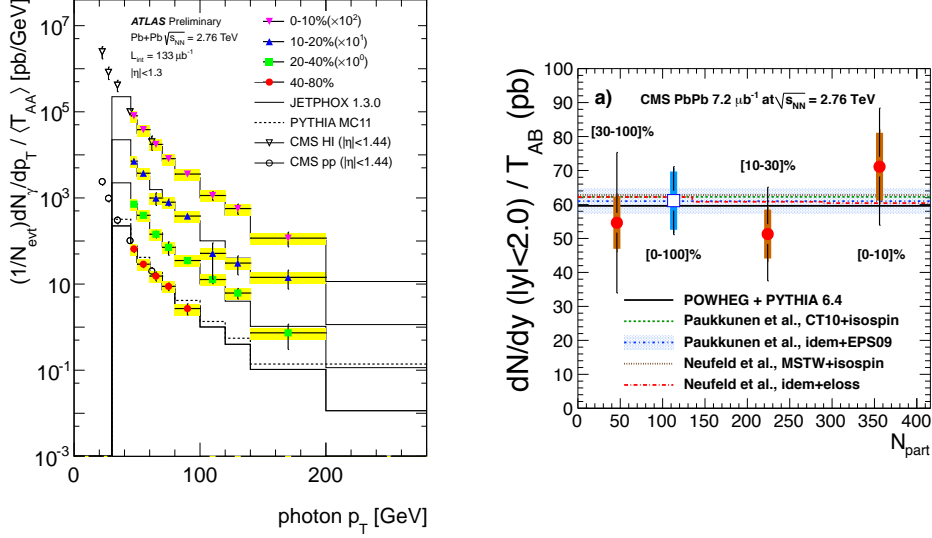


Figure 5. (a, left) Prompt photon p_T spectra measured in Pb+Pb collisions at $\sqrt{s_{NN}}=2.76$ TeV by the ATLAS and CMS experiments together with JETPHOX and PYTHIA simulation [12, 13]. (b, right) Yield of Z-bosons scaled by the nuclear thickness function (T_{AB}) as a function of centrality measured by the CMS experiment [15].

made by utilizing internal conversion of photons [18]. Because these photons decay into e^+e^- , one can use measurement technique for dileptons. The relation between real photon production and the e^+e^- pairs decaying from associated internal conversion photon production can be described as follow [19]:

$$\frac{d^2 n_{ee}}{dm_{ee}} = \frac{2\alpha}{3\pi} \frac{1}{m_{ee}} \sqrt{1 - \frac{4m_e^2}{m_{ee}^2}} \left(1 + \frac{2m_e^2}{m_{ee}^2}\right) S dn_{\gamma}$$

where α is the fine structure constant, m_e and m_{ee} are the masses of the electron and the e^+e^- pair respectively, and S is a process dependent factor that goes to 1 when $m_{ee} \rightarrow 0$ or $m_{ee} \ll p_T$. This equation also applies to the relation between the photons from hadron decays (e.g. $\pi^0 \rightarrow \gamma\gamma$) and the e^+e^- pairs from Dalitz decays ($\pi^0 \rightarrow e^+e^-\gamma$). For π^0 and η , the factor S is given as $S = |F(m_{ee}^2)|^2 (1 - m_{ee}^2/M_h^2)^3$, where M_h is the meson mass and $F(m_{ee}^2)$ is the form factor. The analysis assumes that the form factor for direct photons is $F(m_{ee}^2) = 1$ similar to a purely point-like process. We can select the higher e^+e^- invariant mass region where π^0 contribution becomes off. This will eliminate the large background coming from π^0 Dalitz decay. Figure 6 shows the e^+e^- invariant mass distribution in minimum bias Au+Au collisions for $1.0 < p_T < 1.5$ GeV/c measured by the PHENIX experiment [18]. The e^+e^- mass spectra were fit with the function that have terms of the cocktail calculation of known sources (e^+e^- from various hadron Dalitz decays) and the direct photon internal conversion:

$$f(m_{ee}) = (1 - r)f_c(m_{ee}) + r f_{\text{dir}}(m_{ee})$$

where $f_c(m_{ee})$ is the shape of the cocktail mass distribution, $f_{\text{dir}}(m_{ee})$ is the expected shape of the direct photon internal conversion. One can obtain the signal to background

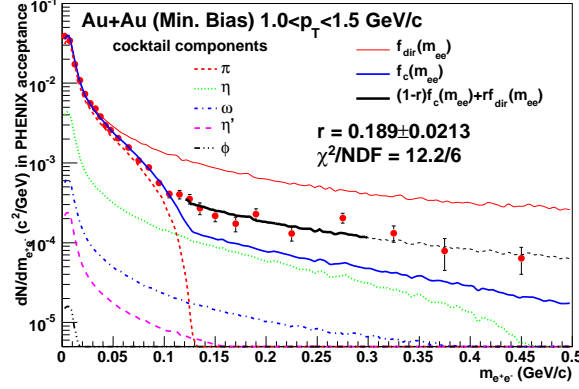


Figure 6. e^+e^- invariant mass distribution at $1.0 < p_T < 1.5$ GeV/c together with the cocktail calculation of known sources and direct photon internal conversion [18].

ratio for a given mass window (r in the plot) at a given p_T . Using the Kroll-Wada formula [20], r is associated with the ratio at zero-mass and thus is converted to the ratio of direct to inclusive photons:

$$r = \frac{\gamma_{\text{dir}}^*(m_{ee} > 0.15)}{\gamma_{\text{inc}}^*(m_{ee} > 0.15)} \propto \frac{\gamma_{\text{dir}}^*(m_{ee} \approx 0)}{\gamma_{\text{inc}}^*(m_{ee} \approx 0)} = \frac{\gamma_{\text{dir}}}{\gamma_{\text{inc}}} \equiv r_\gamma$$

Finally, the direct photon p_T spectra is calculated as $\gamma_{\text{inc}} \times r_\gamma$. Figure 7(a) shows the direct photon p_T spectra in Au+Au and $p + p$ collisions as obtained by this procedure. The spectra were fit with N_{coll} -scaled $p + p$ fit function with exponential function, and

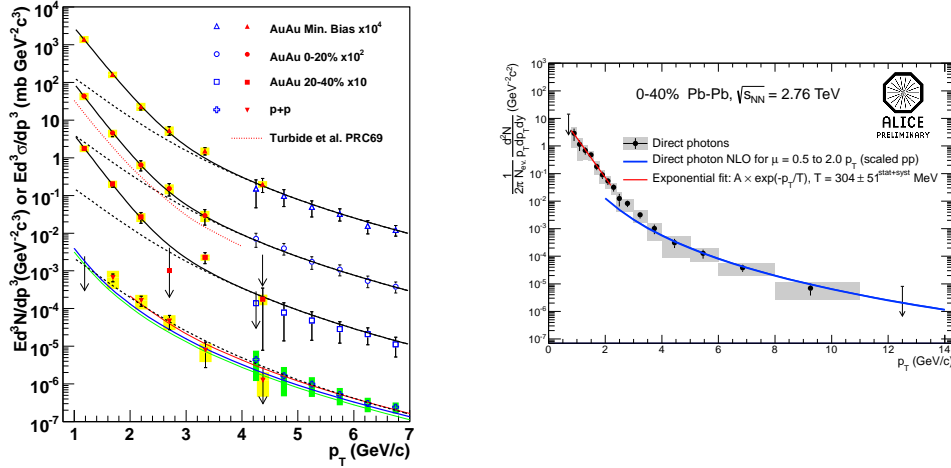


Figure 7. (a, left) PHENIX results on invariant yields of direct photons in Au+Au collisions at various centralities together with that in $p + p$ collisions. Lines show the N_{coll} -scaled $p+p$ fit functions with exponential functions [18]. (b, right) ALICE results on invariant yields of direct photons in 2.76 TeV Pb+Pb collisions [21]

the slope parameters of ~ 220 MeV, which is almost independent of centrality, were ob-

tained. The ALICE experiment recently measured real photons using external conversion technique, namely, by looking at the conversion of real photons into e^+e^- in the material of the inner detectors. Figure 7(b) shows the direct photon p_T spectrum measured by the ALICE experiment in 0-40% Pb+Pb collisions at $\sqrt{s_{NN}}=2.76$ TeV, together with the exponential fit to the low p_T region [21]. The ratio of the slope parameter from PHENIX and ALICE measurements is 1.38. From the published result on the Bjorken energy density at Pb+Pb top centrality from the CMS experiment [22] and one at Au+Au from the PHENIX experiment [23], one can find that the ratio of Bjorken energy density of the LHC Pb+Pb collisions (~ 14 GeV/fm³) to that of RHIC Au+Au (~ 5.7 GeV/fm³) is 2.6, which is smaller than the one expected the ratio of slope parameters ($1.38^4 = 3.65$). This is because the photons measured experimentally are a sum of the photons from all the stages from the initial to the final state of collisions and their slope parameters reflect "average" temperature, while the energy density is measured at the thermalization. In order to obtain the temperature at all the stages as well as the initial energy density, one has to run a hydrodynamical simulation that has a realistic time profile of the system. One might ask if the excess of photons over the initial hard scattering process is due to cold nuclear matter effect (CNM) such as p_T -broadening. PHENIX has recently measured the direct photon production in d +Au collisions to quantify the CNM effect, using the same internal conversion technique applied to Au+Au collisions. Figure 8 shows the R_{AA} of the direct photons in d +Au and Au+Au collisions along with a model on the CNM and parton energy loss effect [24]. It was found that the CNM effect to the direct photon production is negligible compared to the large excess seen in Au+Au collisions.

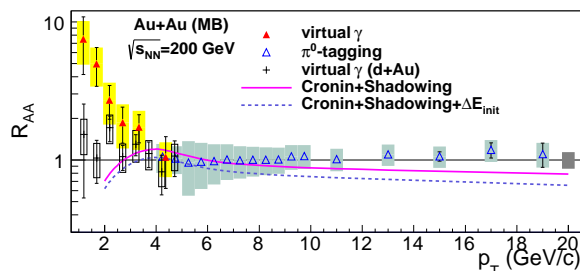


Figure 8. PHENIX results of direct photon R_{AA} in d +Au and Au+Au collisions at $\sqrt{s_{NN}}=200$ GeV [24].

3.2 Flow

After the system reached to local equilibrium, the system proceeds to hydrodynamic expansion and its interaction with hard scattered partons, which results in the anisotropic emission of particles. The magnitude of the anisotropy can be studied from the azimuthal angle distribution of particles relative to the second order event plane angle (v_2 , called as elliptic flow). For particles with low p_T ($p_T < 3$ GeV/ c), the v_2 are understood in terms of pressure-gradient anisotropy in an initial "almond-shaped" collision zone produced in non-central collisions. Recently, a large v_2 of particles and its scaling in terms of kinetic energy have been found for identified charged hadrons at RHIC [25]. It suggested that the system is locally in equilibrium as early as 0.4 fm/ c , and the flow occurs at the partonic level [26]. There are predictions that photons also have a collective motion and their v_2 show different signs and/or magnitudes depending on the production processes [27–29].

The observable is useful to disentangle the contributions from various photon sources in the p_T region where they intermix. The photons from hadron-gas interaction and thermal radiation may follow the collective expansion of a system, and give a positive v_2 . Those photons produced by jet-photon conversion or in-medium Bremsstrahlung will increase as the size of the medium to traverse increases and result in a negative v_2 . The fragment photons will give positive v_2 since larger energy loss of jets is expected in the orthogonal direction to the event plane. PHENIX has measured the v_2 of direct photons by subtracting the v_2 of hadron decay photons off from that of the inclusive photons, following the formula below:

$$v_2^{dir.} = (R \times v_2^{incl.} - v_2^{bkgd.}) / (R - 1), \quad R = (\gamma/\pi^0)_{meas} / (\gamma/\pi^0)_{bkgd}$$

Here, R is obtained either from internal conversion or external conversion method, and $v_2^{incl.}$ is obtained from real photons or their external conversions. Figure 9(a) shows the direct photon v_2 in minimum bias Au+Au collisions at $\sqrt{s_{NN}}=200$ GeV measured by the PHENIX experiment using both internal conversion and external conversion technique [30, 31]. The v_2 of direct photons is sizable and positive, and comparable to the flow

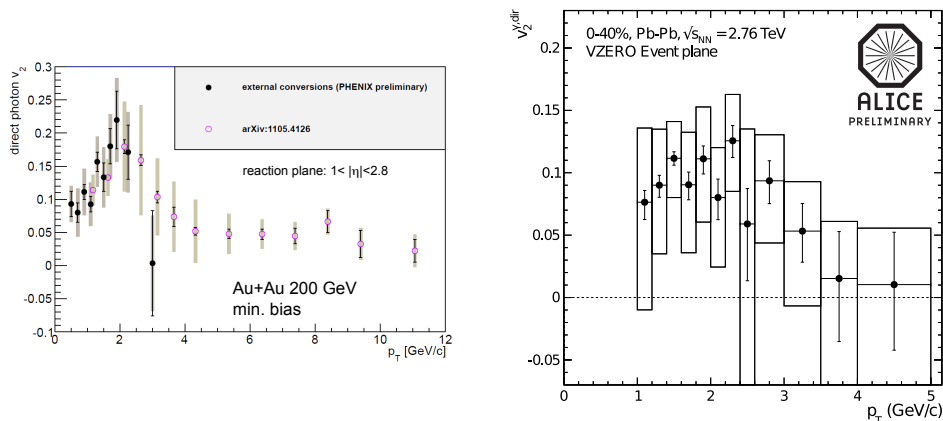


Figure 9. (a, left) Direct photon elliptic flow (v_2) in minimum bias 200 GeV Au+Au collisions measured by the PHENIX experiment, using internal conversion (marked as arXiv:1105.4126) and external conversion technique [30, 31]. (b, right) Direct photon v_2 in 0-40% 2.76 TeV Pb+Pb collisions measured by the ALICE experiment using external conversion technique [32].

of hadrons for $p_T < 3$ GeV/c. The ALICE experiments also obtained the direct photon v_2 in 0-40% Pb+Pb collisions, using external conversion technique recently [32]. Although the energy density and the temperature of the two systems are very different, the v_2 at LHC is surprisingly similar to what PHENIX has found at RHIC.

There are many models that tried explaining the RHIC result. Several models predicted the positive flow of the photons assuming the photons are boosted with hydrodynamic expansion of the system, but the magnitudes from these models are significantly lower than the measurement [33]. There are two models that give relatively large flows. Figure 10 shows a model calculation with increasing photon contribution from hadron-gas interaction [34]. Since the hadrons have a large positive flow as we observed, the photons produced by the interaction with these hadrons result in a large flow. The models (a) and (b) correspond to two ways of incorporating hard photon contribution, namely, a pQCD parametrization and a fit to PHENIX p+p data, respectively. The spectra in low

Photons and dileptons in heavy ion collisions

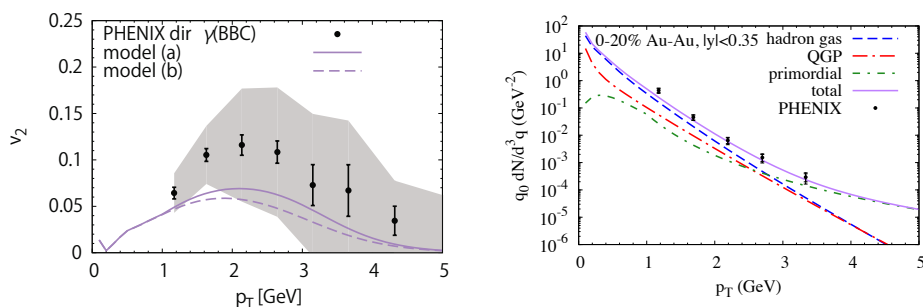


Figure 10. Direct photon v_2 from a theoretical model increasing hadron-gas interaction contribution [34]. (a, left) v_2 from the model calculation, and (b, right) corresponding p_T spectra.

p_T ($1 < p_T < 3 \text{ GeV}/c$) region in this model, where QGP photons are said to dominate, is overwhelmed by the hadron-gas interaction, and QGP contribution is hardly seen. Figure 11 shows a model calculation for direct photon higher order flow (v_n) for two initial conditions, Glauber-based (MCGlb) and CGC-based (MCKLN) conditions, and the corresponding p_T spectrum for the MCGlb case [35, 36]. The shear viscosity is increased

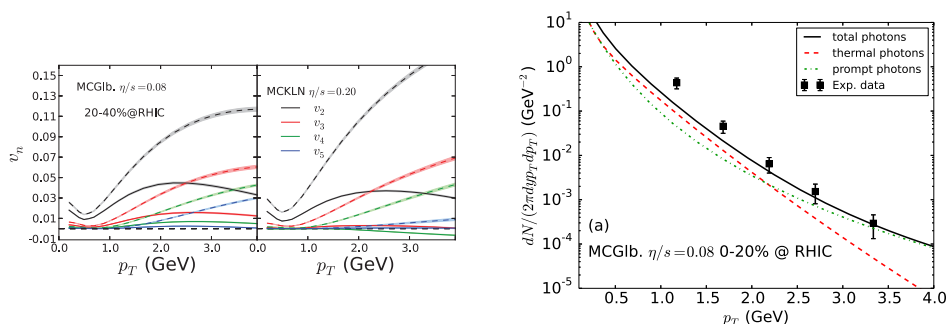


Figure 11. Direct photon v_2 from a theoretical model with including initial state fluctuation and shear viscosity [35, 36]. (a, left) v_2 from the model calculation, and (b, right) corresponding p_T spectra for MCGlb case.

from $\eta/s=0.08$ to 0.20 when switching from MCGlb to MCKLN, in order that the model still describes the flow of hadrons. The dashed and solid lines are before and after viscous corrections are applied on the rates. The reason that this model gives higher values of v_n for MCKLN is that the rate of QGP photons are reduced in order to compensate the viscous entropy production. For a reference, a recent 3+1D hydrodynamic calculation with a new CGC-inspired initial state (IP-Glasma) gives a good description of v_n for charged hadrons at RHIC with shear viscosity of $\eta/s=0.08$ [37]. This implies that the determination of η/s is significantly affected by initial conditions. Both models effectively assume a reduction of QGP photons and call for the hadron-gas photon contribution. Further development at the theory side to explain the data is clearly deserved. Another model tries to explain the large flow by the interaction of photons with the strong magnetic field existing in the non-central collisions [38]. The measurement of triangular flow (v_3) may be useful to discriminate the models; for instance, the strong magnetic field scenario gives $v_3 \sim 0$ while hydrodynamical expansion scenario gives sizable positive v_3 [39].

4. Low mass dileptons

The PHENIX experiment has performed the first measurement of the e^+e^- invariant mass spectra in $p + p$ and Au+Au collisions at $\sqrt{s_{NN}}=200$ GeV at RHIC as shown in Figure 12 [19]. The left panel shows the minimum bias mass spectra with hadronic cocktail

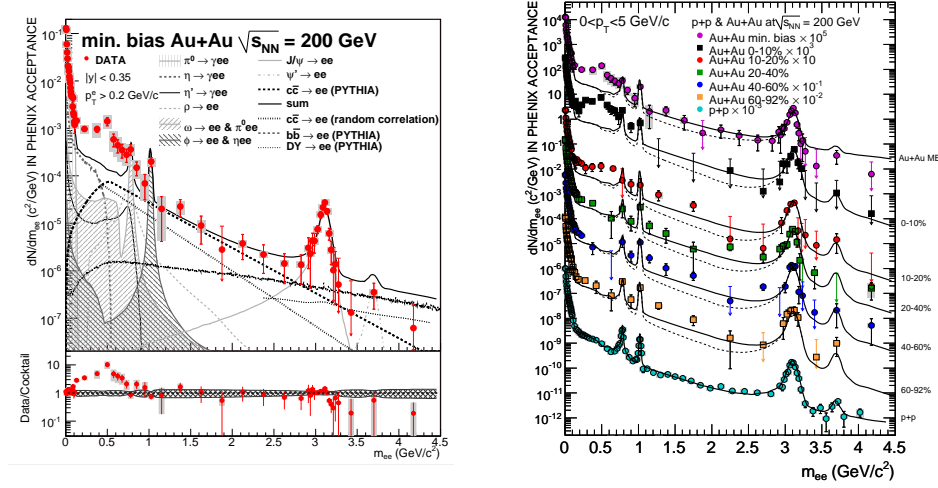


Figure 12. (a, left) e^+e^- mass spectra in minimum bias 200 GeV Au+Au collisions measured by the PHENIX experiments together with cocktail calculation of known sources. (b, right) Centrality dependence of e^+e^- mass spectra and corresponding cocktail calculations for the same dataset [19].

components. The right panel shows the centrality dependence of mass spectra with cocktail calculations. The $p + p$ results are well reproduced by the cocktail of known sources of e^+e^- , whereas the Au+Au data show a strong enhancement at low mass region (LMR, $0.15 < M_{ee} < 0.75$ GeV/ c^2) compared to cocktail calculations. The enhancement for the 0-10% central collisions is a factor of $7.6 \pm 0.5^{stat} \pm 1.3^{syst} \pm 1.5^{model}$ and that for minimum bias collisions is $4.7 \pm 0.4^{stat} \pm 1.5^{syst} \pm 0.9^{model}$, respectively. The STAR experiment also recently obtained e^+e^- mass spectra in $p + p$ and Au+Au collisions at $\sqrt{s_{NN}} = 200$ GeV as shown in Figure 13 [40, 41]. In the same LMR, the enhancement for 0-10% central collisions is $1.72 \pm 0.10 \pm 0.50$, and that for minimum bias collisions is $1.53 \pm 0.07 \pm 0.41$, respectively. Clearly, there is a discrepancy in the magnitudes of the excess by a factor of 3-4 between two experiments. PHENIX has installed a hadron blind detector (HBD) in 2010 run in order to reduce systematic uncertainty of the measurement and also to confirm the previous result. The HBD is a Cherenkov detector with CF4 gas and rejects the e^+e^- tracks from photon conversions and Dalitz decay of π^0 's, which are major background in LMR measurement, by looking at the opening angle of pair tracks in a magnetic field free region [42]. Figure 14(a) shows the e^+e^- mass spectra measured in 20-40% Au+Au collisions in the 2010 run with the HBD [31]. The analysis for the most central collisions are still in progress. PHENIX measurements of 2004 and 2010 have several differences in both data (magnetic field and detector material budget), and cocktail calculations (MC@NLO is used for charm contribution estimate in 2010). PHENIX has made a comparison of the data/cocktail ratio for the integrated yield in LMR obtained in the 2004 and 2010 runs for the three centrality bins as shown in Figure 14(b). It is seen that the two runs give consistent results within uncertainties. It should be noted that the

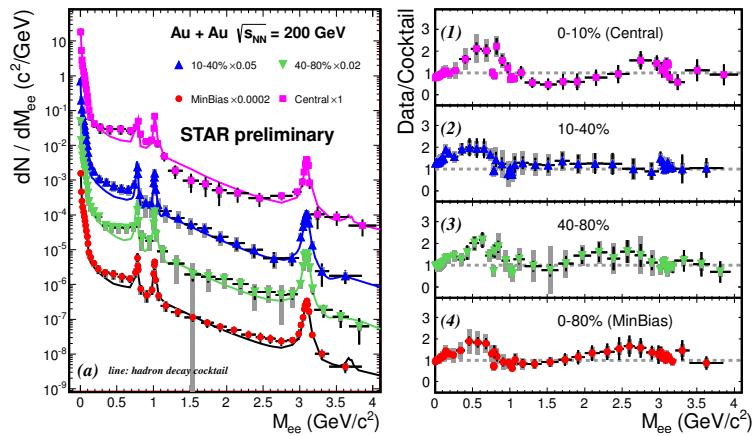


Figure 13. (a, left) e^+e^- mass spectra in various centralities in 200 GeV Au+Au collisions measured by the STAR experiment. (b, right) Ratios of data to cocktail calculation for each centralities [40].

previous PHENIX data showed most of the excess is seen in most central events (0-20%), whose analysis is still in progress. The discrepancy between PHENIX and STAR results persists until PHENIX comes up with the new result with HBD. As for the STAR data, some concern is put on the fact that the cocktail calculation in $p+p$ collisions over-predicts data points in the LMR, though they are still consistent within systematic errors. If one correct for the over-prediction, it is possible STAR and PHENIX see the same amount of excess. Further effort to understand the discrepancy is deserved.

As measured for photons, the measurement of dilepton flow is useful. There is a radial flow measurement of dileptons by the NA60 experiment [43], and an elliptic flow measurement by the STAR experiment [44, 45] that could help disentangling the source of the dileptons that contribute to this particular mass region. A theory study is also in progress [46].

4.1 Energy dependence of LMR dilepton production

The excess in LMR has been explained by various models including in-medium broadening of the ρ mesons or their mass shift [47]. The measurement of the energy dependence of the excess may provide a discrimination of these models. The STAR experiment recently came up with the e^+e^- invariant mass spectra for minimum bias Au+Au collisions at $\sqrt{s_{NN}} = 19.6, 62.4,$ and 200 GeV as shown in Figure 15 [40]. STAR observed a qualitatively similar excess as observed by the CERES measurements in the Pb+Au at $\sqrt{s_{NN}} = 17.2$ GeV [48]. In each of the three panels the hadron cocktail simulation includes contributions from Dalitz decays, photon conversions (19.6 GeV only), and the dielectron decay of the ω and ϕ vector mesons. The cocktail simulations purposely exclude contributions from ρ mesons. Instead, these are explicitly included in the model calculation by Rapp [47] which involve in-medium modifications of the ρ meson spectral shape in the isentropic fireball evolution. The LMR enhancement measured by STAR are consistently agreeing with these model calculations within the quoted errors. One should be careful on taking the absolute magnitude of the excess in all energies, provided that there is still the issue of inconsistency between STAR and PHENIX. Nonetheless, it is

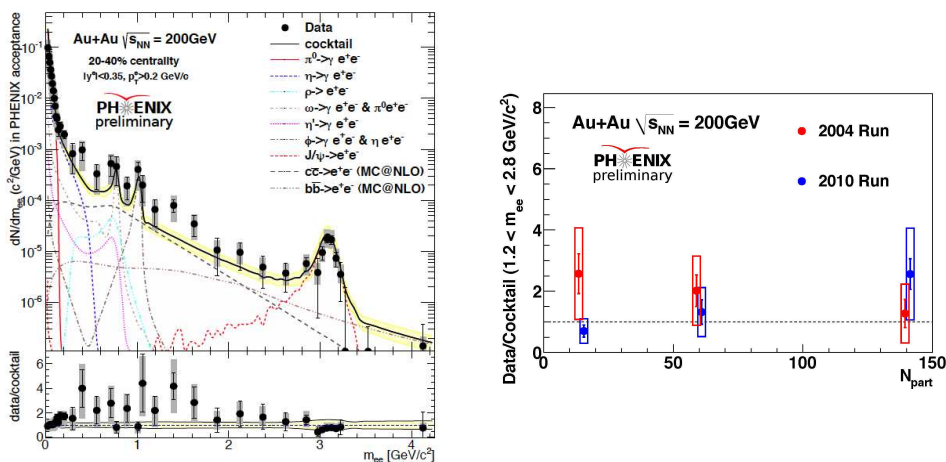


Figure 14. (a, left) e^+e^- mass spectra in 20-40% Au+Au collisions measured by the PHENIX experiment in 2010, with a hadron blind detector (HBD) installed. (b, right) Comparison of the ratio of the integrated yields in the LMR to the cocktail calculations in 2004 and 2010 dataset [31].

interesting to see that the relative change as a function cms energy is well described by this model calculation. If it is the case, the flow of this mass region may exhibit the KE_T scaling with assuming they are all ρ .

5. Summary

The recent results on direct photons and dileptons in high energy heavy ion collisions, obtained particularly at RHIC and LHC are reviewed. The results are new not only in terms of the probes, but also in terms of the precision. Much progress has been made in understanding high p_T direct photons as well as Z -bosons with the latest RHIC and LHC results. The soft single photons have been studied down to lower p_T using internal conversion and external conversion technique at RHIC and LHC, and exhibit the average temperature of the system. A large flow of soft photons was also observed both at RHIC and LHC, which are not explained by models considering QGP only so far. The low mass dilepton excess was observed at the PHENIX and STAR experiments at RHIC in Au+Au collisions, but are not quantitatively agreeing each other. The flow of dilepton is as important as the one of photons, and experiments should make an effort to improve the measurement. The STAR results on dileptons at several cms energies shows that the excess in LMR is consistent with in-medium modification of the ρ meson spectral function. If it is the case, the flow of this mass region may exhibit the KE_T scaling with assuming they are all ρ . This is an interesting topic to explore.

References

- [1] See for example, J-e. Alam, S. Raha, B. Sinha, Phys. Rep. 273 (1996) 243.
- [2] L. E. Gordon and W. Vogelsang, Phys. Rev. D **48**, 3136 (1993).
- [3] S. Turbide, R. Rapp and C. Gale, Phys. Rev. C **69**, 014903 (2004).
- [4] R. J. Fries, B. Muller and D. K. Srivastava, Phys. Rev. C **72**, 041902 (2005).
- [5] A. Adare *et al.* [PHENIX Collaboration], Phys. Rev. C **87**, 034911 (2013).

Photons and dileptons in heavy ion collisions

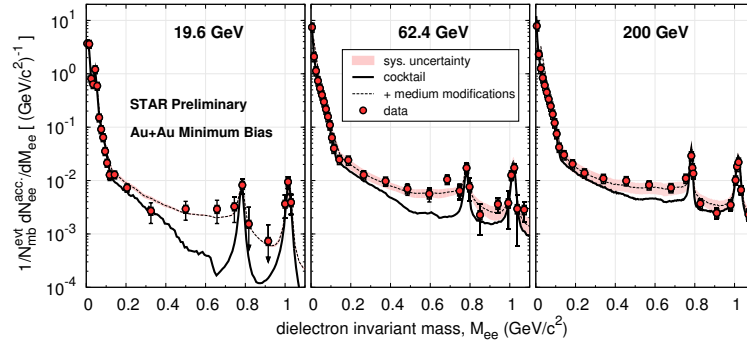


Figure 15. e^+e^- mass spectra measured by the STAR experiment in 19.6, 62.4 and 200 GeV Au+Au collisions, together with cocktail calculation and a theoretical model assuming in-medium modification of ρ spectral function [40].

- [6] M. M. Aggarwal *et al.* [WA98 Collaboration], Phys. Rev. Lett. **85**, 3595 (2000).
- [7] R. Rapp, Phys. Rev. C **63**, 054907 (2001) [Phys. Rev. A **83**, 043833 (2011)]
- [8] A. Drees, Nucl. Phys. A **830**, 435C (2009).
- [9] S. S. Adler *et al.* [PHENIX Collaboration], Phys. Rev. Lett. **94**, 232301 (2005).
- [10] S. Afanasiev *et al.* [PHENIX Collaboration], Phys. Rev. Lett. **109**, 152302 (2012).
- [11] F. Arleo, JHEP **0609**, 015 (2006).
- [12] P. Steinberg [ATLAS Collaboration], Nucl. Phys. A **904-905**, 233c (2013).
- [13] S. Chatrchyan *et al.* [CMS Collaboration], Phys. Lett. B **710**, 256 (2012).
- [14] A. Adare *et al.* [PHENIX Collaboration], Phys. Rev. Lett. **111**, 032301 (2013).
- [15] S. Chatrchyan *et al.* [CMS Collaboration], Phys. Rev. Lett. **106**, 212301 (2011).
- [16] G. Aad *et al.* [ATLAS Collaboration], Phys. Rev. Lett. **110**, 022301 (2013).
- [17] S. Chatrchyan *et al.* [CMS Collaboration], JHEP **1305**, 090 (2013).
- [18] A. Adare *et al.* [PHENIX Collaboration], Phys. Rev. Lett. **104**, 132301 (2010).
- [19] A. Adare *et al.* [PHENIX Collaboration], Phys. Rev. C **81**, 034911 (2010).
- [20] N. M. Kroll and W. Wada, Phys. Rev. **98**, 1355 (1955).
- [21] M. Wilde [ALICE Collaboration], Nucl. Phys. A **904-905**, 573c (2013).
- [22] S. Chatrchyan *et al.* [CMS Collaboration], Phys. Rev. Lett. **109**, 152303 (2012).
- [23] S. S. Adler *et al.* [PHENIX Collaboration], Phys. Rev. C **71**, 034908 (2005) [Erratum-ibid. C **71**, 049901 (2005)].
- [24] A. Adare, *et al.* [PHENIX Collaboration], Phys. Rev. C **87**, 054907 (2013).
- [25] See for example, A. Adare *et al.* [PHENIX Collaboration], Phys. Rev. Lett. **98**, 162301 (2007).
- [26] B. Schenke, S. Jeon and C. Gale, Phys. Rev. C **82**, 014903 (2010).
- [27] S. Turbide, C. Gale and R. J. Fries, Phys. Rev. Lett. **96**, 032303 (2006).
- [28] R. Chatterjee, E. S. Frodermann, U. W. Heinz and D. K. Srivastava, Phys. Rev. Lett. **96**, 202302 (2006).
- [29] S. Turbide, C. Gale, E. Frodermann and U. Heinz, Phys. Rev. C **77**, 024909 (2008).
- [30] A. Adare *et al.* [PHENIX Collaboration], Phys. Rev. Lett. **109**, 122302 (2012).
- [31] I. Tserruya [PHENIX Collaboration], Nucl. Phys. A **904-905**, 225c (2013).
- [32] D. Lohner [ALICE Collaboration], J. Phys. Conf. Ser. **446**, 012028 (2013).
- [33] R. Chatterjee and D. K. Srivastava, Nucl. Phys. A **830**, 503C (2009).
- [34] H. van Hees, C. Gale and R. Rapp, Phys. Rev. C **84**, 054906 (2011).
- [35] C. Shen, U. W. Heinz, J. -F. Paquet, I. Kozlov and C. Gale, arXiv:1308.2111 [nucl-th].
- [36] C. Shen, U. W. Heinz, J. -F. Paquet and C. Gale, arXiv:1308.2440 [nucl-th].
- [37] C. Gale, S. Jeon, B. Schenke, P. Tribedy and R. Venugopalan, Phys. Rev. Lett. **110**, 012302 (2013).
- [38] See for example, A. Bzdak and V. Skokov, Phys. Rev. Lett. **110**, 192301 (2013).

T. Sakaguchi

- [39] See for example, R. Chatterjee, D. K. Srivastava and T. Renk, arXiv:1401.7464 [hep-ph].
- [40] F. Geurts [STAR Collaboration], Nucl. Phys. A904-905 **2013**, 217c (2013).
- [41] L. Adamczyk *et al.* [STAR Collaboration], arXiv:1312.7397 [hep-ex].
- [42] W. Anderson, B. Azmoun, A. Cherlin, C. Y. Chi, Z. Citron, M. Connors, A. Dubey and J. M. Durham *et al.*, Nucl. Instrum. Meth. A **646**, 35 (2011).
- [43] R. Arnaldi *et al.* [NA60 Collaboration], Phys. Rev. Lett. **100**, 022302 (2008).
- [44] X. Cui [STAR Collaboration], J. Phys. Conf. Ser. **446**, 012047 (2013).
- [45] L. Adamczyk *et al.* [STAR Collaboration], arXiv:1402.1791 [nucl-ex].
- [46] G. Vujanovic, C. Young, B. Schenke, R. Rapp, S. Jeon and C. Gale, arXiv:1312.0676 [nucl-th].
- [47] See for example, R. Rapp and J. Wambach, Eur. Phys. J. A **6**, 415 (1999).
- [48] G. Agakichiev *et al.* [CERES Collaboration], Eur. Phys. J. C **41**, 475 (2005).